

SCIENTIFIC REPORTS



OPEN

Grayscale image recording on $\text{Ge}_2\text{Sb}_2\text{Te}_5$ thin films through laser-induced structural evolution

Tao Wei^{1,2}, Jingsong Wei³, Kui Zhang^{2,3}, Hongxia Zhao³ & Long Zhang¹

Received: 04 October 2016
 Accepted: 13 January 2017
 Published: 14 February 2017

Chalcogenide $\text{Ge}_2\text{Sb}_2\text{Te}_5$ thin films have been widely exploited as binary bit recording materials in optical and non-volatile electronic information storage, where the crystalline and amorphous states are marked as the information bits "0" and "1", respectively. In this work, we demonstrate the use of $\text{Ge}_2\text{Sb}_2\text{Te}_5$ thin films as multi-level grayscale image recording materials. High-resolution grayscale images are recorded on $\text{Ge}_2\text{Sb}_2\text{Te}_5$ thin films through taking advantage of laser-induced structural evolution characteristic. Experimental results indicate that the change of laser energy results in the structural evolution of $\text{Ge}_2\text{Sb}_2\text{Te}_5$ thin films. The structural evolution induces the difference of electronic polarizability and reflectivity, and high-resolution grayscale images are recorded on $\text{Ge}_2\text{Sb}_2\text{Te}_5$ thin films through direct laser writing method, accordingly.

The binary bit encoding is extensively exploited in traditional optical data storage¹. However, the binary bit encoding actually has the disadvantages of low storage density and complex encoding transfer for read-out. For example, when an image is stored by binary encoding method, the storage capacity of several gigabits is generally required. In contrast, if the image can be recorded through multi-level bit data encoding method, the capacity may be improved greatly compared with traditional binary encoding method^{2,3}. The multi-level bit encoding can be realized through direct grayscale recording^{4,5}. Moreover, the grayscale image recording has the advantage of facile writing and readout without the transcoding process. Chalcogenide $\text{Ge}_2\text{Sb}_2\text{Te}_5$ thin films, possessing good thermal stability and large number of achievable rewriting cycles^{6–9}, have been successfully applied in binary bit encoding data storage by taking advantage of the optical reflectivity contrast between the crystalline and amorphous states induced by laser pulse radiation^{6,10,11}. $\text{Ge}_2\text{Sb}_2\text{Te}_5$ thin films have also been used for fluorescence phase-change multilevel recording medium¹². Recently, Wang, *et al.* demonstrated high-density multi-level crystallization of a $\text{Ge}_2\text{Sb}_2\text{Te}_5$ thin film by adjusting focused femtosecond laser pulse number¹³. Moreover, grayscale images were written into the storage medium. However, details of structure revolution are less reported for grayscale image recording.

$\text{Ge}_2\text{Sb}_2\text{Te}_5$ thin film is used as our grayscale recording material, which has the crystallization temperature of about 160 °C¹³. Low laser energy is required for grayscale recording. Moreover, large change of optical reflectivity of $\text{Ge}_2\text{Sb}_2\text{Te}_5$ thin film is also beneficial for the realization of colorful grayscale⁶. Our prior work reported the use of Sb_2Te_3 thin film as grayscale recording material⁴. The formation of grayscale image is due to different height and size of bump structure. In this work, it is found that the change of laser energy can result in the evolution of chemical bonds of $\text{Ge}_2\text{Sb}_2\text{Te}_5$ thin films, which induces the difference of electronic polarizability and then reflectivity change. Thus, multi-level bit encoding features can be easily generated only by tuning laser energy, and one can obtain the grayscale image recording on $\text{Ge}_2\text{Sb}_2\text{Te}_5$ thin films through taking advantage of the laser-induced structural evolution. Arbitrary images such as tiger, dog and flowers have been successfully recorded on $\text{Ge}_2\text{Sb}_2\text{Te}_5$ thin films by direct laser writing method.

Experimental Details

The $\text{Ge}_2\text{Sb}_2\text{Te}_5$ thin film deposited on a K9 glass substrate with the thickness of 100 nm was prepared by radio frequency magnetron controlling sputtering system (JGP560 type) at room temperature, in which the background

¹Key Laboratory of Materials for High Power Laser, Shanghai Institute of Optics and Fine Mechanics, Chinese Academy of Sciences, Shanghai 201800, PR China. ²University of Chinese Academy of Sciences, Beijing 100049, People's Republic of China. ³Laboratory for High Density Optical Storage, Shanghai Institute of Optics and Fine Mechanics, Chinese Academy of Sciences, Shanghai 201800, PR China. Correspondence and requests for materials should be addressed to J.W. (email: weijingsong@siom.ac.cn) or L.Z. (email: lzhong@siom.ac.cn)

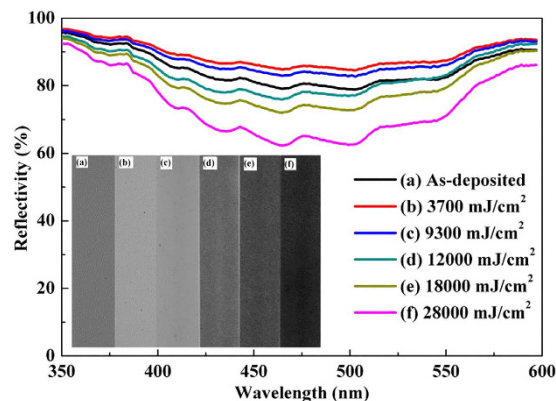


Figure 1. Reflective spectra (inset: multi-level grayscale tones) of $\text{Ge}_2\text{Sb}_2\text{Te}_5$ thin films at the irradiation of various laser energy densities, (a) as-deposited state; (b) 3700 mJ/cm^2 ; (c) 9300 mJ/cm^2 ; (d) 12000 mJ/cm^2 ; (e) 18000 mJ/cm^2 ; (f) 28000 mJ/cm^2 .

pressure was approximately $7.5 \times 10^{-4} \text{ Pa}$, the sputtering power was 30 W and the working gas was Ar gas with the pressure of 0.5 Pa.

The grayscale image recording was obtained by direct laser writing system (LASERWRITER LW405B+) with the laser wavelength of 405 nm and the numerical aperture (NA) of 0.65 for focusing lens. The recorded spot diameter was theoretically 760 nm based on the diffraction limit formula $D = 1.22 \times \lambda / \text{NA}$, where D was diameter of spot; λ was laser wavelength and NA was numerical aperture of focusing lens. In practice, the spot size was $1 \mu\text{m}$ due to the imperfect optical system. The image recording processes are as follows: the grayscale values of each pixel of original pictures are read by computer program. Afterwards, each grayscale value corresponds to a laser power value. Then computer program controls the laser power of each pixel by grayscale values. Thus, arbitrary grayscale patterns are fabricated by continuously adjustable laser power value. In writing process, beam scanning mode was utilized, that is, laser beam moved on the sample surface by raster scanning and performed scanning writing in line by line. X-ray diffraction (XRD) data were recorded via 18KW-D/MAX2500V type equipment produced by Rigaku. The fabricated grayscale patterns were observed by optical microscope (Olympus BX51 microscopy) with white light source illumination. In order to investigate the mechanism of multi-level grayscale image recording, micro-reflection and Raman spectra between laser-irradiated and un-irradiated regions were obtained by reflection spectrum (PG2000-Pro, Idea Optics Company, China) and Renishaw Micro-Raman Spectroscopy System with the excitation wavelength of 532 nm, respectively. X-ray photoelectron spectroscopy (XPS) measurement was performed by an XPS spectrometer (Microlab 310F) produced by VG Scientific and the exciting source is $\text{Mg K}\alpha$. Optical constant of prepared $\text{Ge}_2\text{Sb}_2\text{Te}_5$ layers were obtained from the analysis of spectroscopic ellipsometry data measured using an ellipsometer with an automatic rotating analyzer (VASE, J. A. Woollam Co., Inc.). All measurements were carried out at room temperature.

Results and Discussion

Multi-level grayscale features. For the purpose of achieving grayscale image recording on $\text{Ge}_2\text{Sb}_2\text{Te}_5$ thin films, multi-level grayscale characteristics are obtained by tuning laser energy density. Moreover, reflective spectra are determined as can be seen in Fig. 1, where Al mirror is firstly used to correct the base reflectivity and its reflectivity is set to 100%. It can be observed from the inset of Fig. 1 that with increasing laser energy from 0 to 3700 mJ/cm^2 , the color of $\text{Ge}_2\text{Sb}_2\text{Te}_5$ thin film becomes lighter and then it becomes darker when further increasing laser energy from 3700 mJ/cm^2 to 28000 mJ/cm^2 . From reflective spectra one can see that when the laser energy is 3700 mJ/cm^2 , the reflectivity reaches the maximum and further increase of laser energy density from 3700 mJ/cm^2 to 28000 mJ/cm^2 leads to gradual reduction of reflectivity. The reflectivity difference can be as high as 20%, which in turn may generate large optical contrast. Results suggest that multi-level grayscale tones can be determined by finely tuning laser energy and $\text{Ge}_2\text{Sb}_2\text{Te}_5$ thin film is a promising candidate material for grayscale image recording. It is noted that the grayscale in Fig. 1f becomes black while corresponding lowest reflectivity still reaches to 60%. This may be due to the fact that strong light source illumination in optical microscopy generates strong mirror reflection and high reflectivity. Further study will be performed to increase absolute contrast for the applications of real image recording.

Laser induced structural evolution characteristic. *X-ray diffraction analysis.* Figure 2 shows the X-ray diffraction patterns of $\text{Ge}_2\text{Sb}_2\text{Te}_5$ thin films. It can be seen that only a small mountain peak centered at 28° is observed in as-deposited $\text{Ge}_2\text{Sb}_2\text{Te}_5$ thin film, indicating that the prepared thin film is almost amorphous state. After the laser energy irradiation, the $\text{Ge}_2\text{Sb}_2\text{Te}_5$ thin film with obvious diffraction peaks is determined, which corresponds to a typically metastable face-centered cubic crystal¹⁴. Moreover, the diffraction peaks become stronger with the increment of laser energy density from 3700 to 12000 mJ/cm^2 . However, when the laser energy further increases to 28000 mJ/cm^2 , the diffraction peaks become weaker gradually. This phenomenon is similar to other reports¹⁵ and can be explained that the thin film is excessively ablated after the laser irradiation and then transformed back to an amorphous state due to high laser energy density.

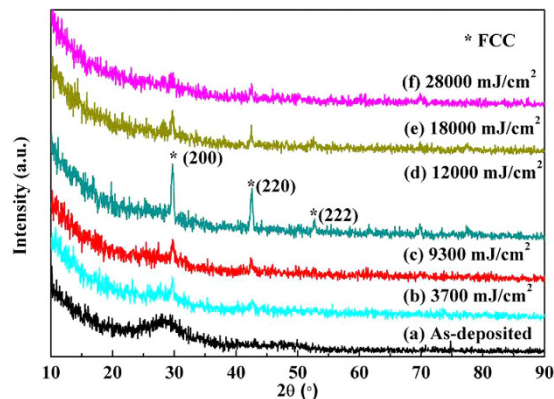


Figure 2. X-ray diffraction patterns of the $\text{Ge}_2\text{Sb}_2\text{Te}_5$ thin films with various laser energy irradiations, where (a) as-deposited state; (b) 3700 mJ/cm^2 ; (c) 9300 mJ/cm^2 ; (d) 12000 mJ/cm^2 ; (e) 18000 mJ/cm^2 and (f) 28000 mJ/cm^2 .

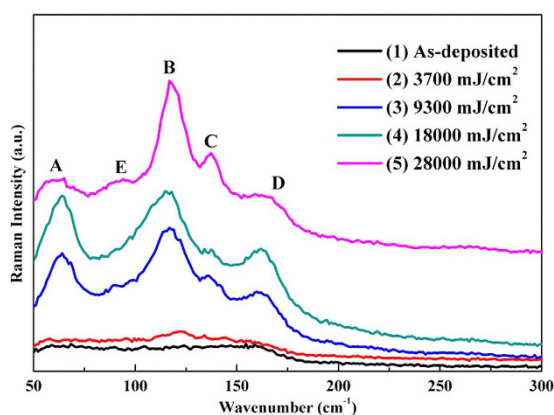


Figure 3. Raman spectra of $\text{Ge}_2\text{Sb}_2\text{Te}_5$ thin films with the irradiation of various energy densities: (1) as-deposited sample; (2) 3700 mJ/cm^2 ; (3) 9300 mJ/cm^2 ; (4) 18000 mJ/cm^2 ; (5) 28000 mJ/cm^2 .

Raman spectra analysis. To further characterize the structure changes, Raman spectra of laser-irradiated $\text{Ge}_2\text{Sb}_2\text{Te}_5$ thin films are measured as shown in Fig. 3. One can see that the as-deposited thin film shows a broad peak around 150 cm^{-1} which is a characteristic peak for amorphous $\text{Ge}_2\text{Sb}_2\text{Te}_5$ film and normally ascribed to the stretching vibration of amorphous Te–Te bond^{14,16,17}. After the laser irradiation, the broad peak at 150 cm^{-1} is gradually divided into several peaks marked as ‘A’, ‘B’, ‘C’ and ‘D’. Raman peak ‘A’ is located at 64 cm^{-1} , which is very similar to other reports and can be assigned to the vibration of 3-fold coordinated Te^{18,19}. The peaks ‘B’ at 117 cm^{-1} are very similar to the results in ref. 20, in which the Raman peak is located at 120 cm^{-1} and assigned to A_1 symmetry of corner-sharing $\text{GeTe}_{4-n}\text{Ge}_n$ ($n = 0, 1, 2, 3$) tetrahedral units^{14,15,21,22}. The difference may be caused by the vibration of heteropolar bonds in GeTe_4 or $\text{GeTe}_3\text{Ge}^{15}$. The peak ‘C’ at 137 cm^{-1} may be attributed to the segregation of Te crystalline phase for over-irradiation¹⁴. The peak ‘D’ at 160 cm^{-1} can be ascribed to the $A_{1g}(2)$ vibration of crystalline Sb_2Te_3 ¹⁵.

With increasing laser energy from 3700 to 28000 mJ/cm^2 , the vibrational peaks at 117 cm^{-1} and 137 cm^{-1} become stronger gradually. However, the peak at 160 cm^{-1} becomes weaker and has been dramatically suppressed when the laser energy is up to 28000 mJ/cm^2 . This indicates that the formation of Te crystal is at the expense of crystalline Sb_2Te_3 , and leads to a large suppression of peak at 160 cm^{-1} . Besides, when laser energy is up to 28000 mJ/cm^2 , a new Raman peak ‘E’ at 90 cm^{-1} can be observed, which is due to the E mode of GeTe_4 tetrahedral²².

XPS spectra analysis. XPS was used for the determination of the binding state of each component as Ge, Sb and Te. Figure 4a displays XPS spectra of Ge $2p_{3/2}$. One can see a main peak at 1218 eV , which is assigned to Ge–Sb or Ge–Te metallic bonds in as-deposited $\text{Ge}_2\text{Sb}_2\text{Te}_5$ thin films^{23,24}. With increasing the irradiation of laser energy, the main peak position moves to 1219 eV , indicating the formation Ge–O bonds²⁴. Moreover, the signal intensity of Ge–O bond increases to the maximum when the laser energy is up to 12000 mJ/cm^2 . However, further increment of laser energy leads to weaker Ge–O bond signal and stronger Ge–Sb or Ge–Te bond signals.

Figure 4b shows XPS spectra of Sb $3d$ at the irradiation of various laser energy densities. For the as-deposited sample, there are four peaks at 528.48 eV , 530.28 eV for Sb $3d_{5/2}$ and 537.78 eV , 539.48 eV for Sb $3d_{3/2}$, respectively. Among them, the peaks at 528.48 eV and 537.78 eV are ascribed to the homopolar (Sb–Sb) bonds while peaks at 530.28 eV and 539.48 eV are due to the Sb–O bonds due to the strong surface oxidation effects^{25,26}. With increasing

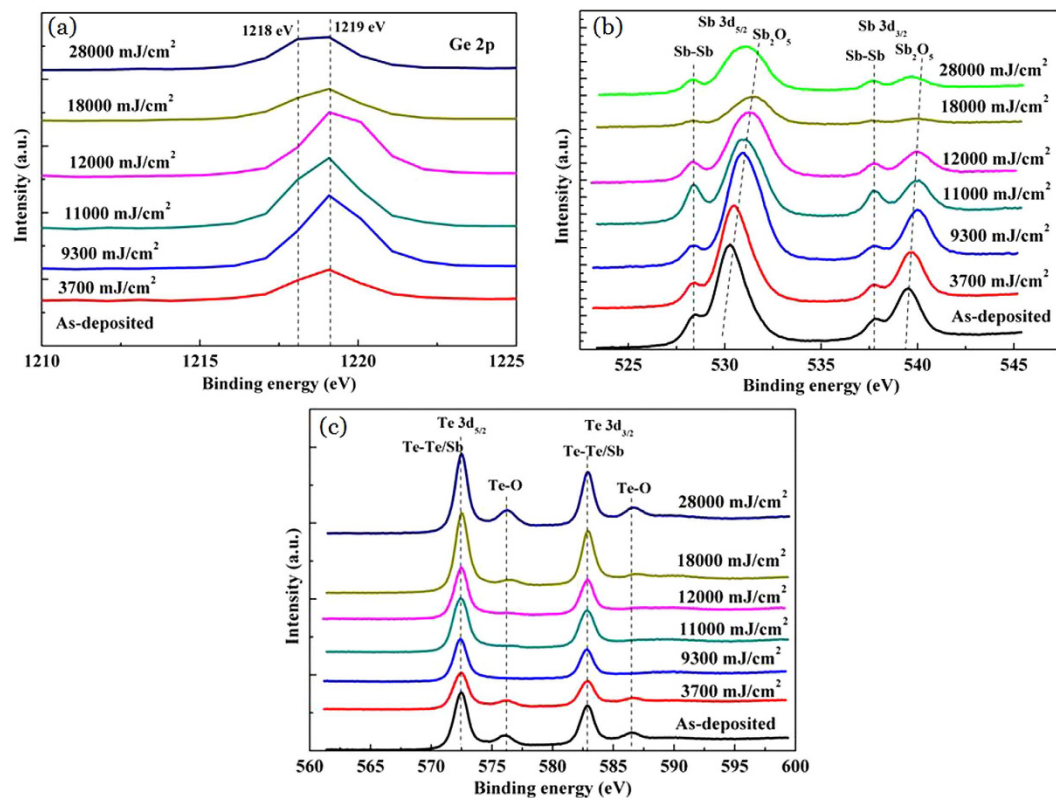


Figure 4. XPS spectra at the irradiation of various laser energy densities; (a) Ge 2p, (b) Sb 3d, (c) Te 3d.

laser energy, the signals of Sb-Sb bonds become stronger. When laser energy density is up to 12000 mJ/cm^2 , the intensity of Sb-Sb bond reaches the maximum, which indicates that Sb homopolar bonds play an important role to maintain overall structure stability in crystalline phase. However, further increasing laser energy causes weaker signals of Sb-Sb bonds. In addition, the peak of Sb-O bond moves to higher energy region with the increment of laser energy, which may result in multi-level grayscale on $\text{Ge}_2\text{Sb}_2\text{Te}_5$ thin films due to obvious structural changes.

The XPS spectra of Te 3d are depicted in Fig. 4c. In general, the peaks located at $572.5\text{--}574 \text{ eV}$ and $583\text{--}584 \text{ eV}$ were related to Te metallic bonds²⁵. However, in our work, the peaks of metallic bonds are located at 572.48 eV and 582.88 eV , respectively. This may be ascribed to Sb-Te and Te-Te bonds^{25,26}. When laser energy increases, the Te metallic bonds have no evident changes. Additionally, the binding energies peaks at 576.28 eV and 586.68 eV both correspond to Te-O bonds²⁶. It can be seen that the peaks of Te-O bonds gradually become weaker as laser energy increases and then disappear totally at the laser energy of $9300\text{--}12000 \text{ mJ/cm}^2$. Further increment of laser energy leads to the formation of Te-O bonds, again. The disappearance of Te-O bonds can be due to that Te atoms participate in the formation and growth of crystalline $\text{Ge}_2\text{Sb}_2\text{Te}_5$ thin films.

Spectroscopic ellipsometry analysis. In order to more intuitively understand the chemical bonding origin of optical contrast between as-deposited state and laser irradiated regions, spectroscopic ellipsometry data are determined and wavelength dependent dielectric functions, refractive index and extinction coefficient are shown in Fig. 5. The detailed data processing can be found elsewhere^{21,27}. It can be seen from Fig. 5(a and b) that the dielectric functions show a single peak due to bonding–antibonding transitions¹⁰. Furthermore, ϵ has substantial differences at peak position and peak shape between as-deposited state and laser irradiated regions. Moreover, with changing laser energy, ϵ also has evident changes, which indicates that electronic polarizability and chemical bonds vary with tuning laser energy density^{10,28,29}. In parallel, the refractive index and extinction coefficient change substantially with adjusting laser energy as revealed in Fig. 5(c and d). This in turn brings about the evolution of optical reflectivity. However, the tendency of refractive index and extinction coefficient change is in poor agreement with the trend of optical reflectivity change. It may be explained that the optical reflectivity is determined by the combination of refractive index and extinction coefficient. Therefore, it is proposed that multi-level grayscale image recording may be realized by tuning laser energy.

Multi-level grayscale image recording. According to tuning laser energy, multi-level grayscale image recording can be achieved. The arbitrary multi-level grayscale images are recorded on $\text{Ge}_2\text{Sb}_2\text{Te}_5$ thin films as shown in Fig. 6. The grayscale levels used in the recorded grayscale images were reached to 256 levels. It is noted that the laser energy density ranges from 0 to 93000 mJ/cm^2 . Figure 6(b and d) show the lifelike flowers, in which the details can be presented clearly and very similar to original pictures as shown in Fig. 6(a and c). In addition, Fig. 6(e and f) present dog and tiger images recorded on the $\text{Ge}_2\text{Sb}_2\text{Te}_5$ thin film, respectively. Figure 6(e) displays

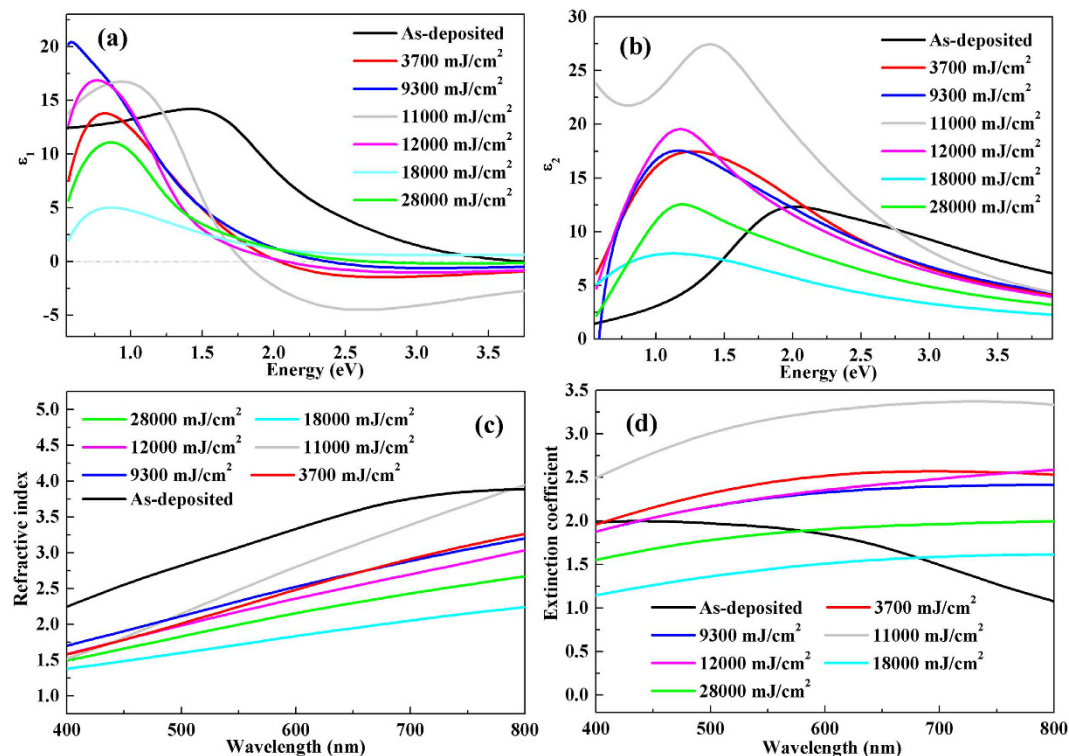


Figure 5. The (a) real (ϵ_1) and (b) imaginary (ϵ_2) part of the dielectric functions; (c) refractive index and (d) extinction coefficient in $\text{Ge}_2\text{Sb}_2\text{Te}_5$ thin films at the irradiation of various laser energy densities.

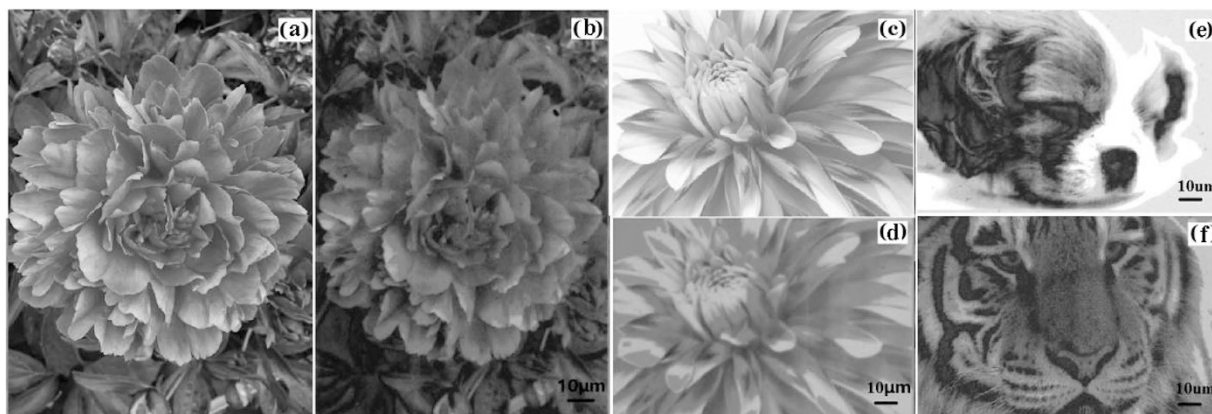


Figure 6. Grayscale patterns written on $\text{Ge}_2\text{Sb}_2\text{Te}_5$ thin films with the energy density of 93000 mJ/cm^2 , where (a) and (c) are original pictures and (b), (d–f) are recording grayscale images. It is noted that (a–d) are flowers; (e, f) are dog and tiger patterns.

recorded patterns of the sleeping dog. The expression and appearance of the sleeping dog can be clearly recorded on the $\text{Ge}_2\text{Sb}_2\text{Te}_5$ thin film. Besides, one can see from Fig. 6(f) that the expression and appearance of the lifelike tiger are fully recorded onto $\text{Ge}_2\text{Sb}_2\text{Te}_5$ thin films by precisely controlling the laser energy density, which can be observed from some fine structures like eyes, furs and whiskers. It is worthwhile mentioning that the regions in Fig. 6(c) appear brightest; however the corresponding regions in Fig. 6(d) appear darker. This is due to that the laser energy density is not optimal. Further optimization of laser energy density will be performed to obtain more lifelike grayscale images. Results demonstrate that $\text{Ge}_2\text{Sb}_2\text{Te}_5$ thin film is a promising multi-level grayscale image recording material for applications of high-resolution grayscale image storage.

Conclusions

In summary, we demonstrate that the change of laser energy results in the structural evolution of $\text{Ge}_2\text{Sb}_2\text{Te}_5$ thin films. The structural evolution induces the difference of electronic polarizability and then reflectivity change.

It is found that the reflectivity increases with enhancing crystallization extent of $\text{Ge}_2\text{Sb}_2\text{Te}_5$ thin film; however, further increasing laser energy leads to the molten state of thin films and lower reflectivity. The combination of amorphous, crystallization and molten state generates colorful grayscale levels. The multi-level bit encoding features can be generated only by tuning laser irradiation energy. The grayscale image recording on $\text{Ge}_2\text{Sb}_2\text{Te}_5$ thin films can be obtained through taking advantage of the laser-induced structural evolution, accordingly. Arbitrary images have been successfully recorded on $\text{Ge}_2\text{Sb}_2\text{Te}_5$ thin films, which indicate that $\text{Ge}_2\text{Sb}_2\text{Te}_5$ thin film is a promising candidate for applications of high-resolution grayscale image storage.

References

1. Fumio, K. Binary encoding method for data read from optical record and device. *United States Patent No.* 4819222 (1989).
2. Zhou, T. R. *et al.* Multilevel amplitude-modulation system for optical data storage. *Proc. SPIE* **4930**, 7–20 (2002).
3. Xie, C., Liu, C., Wang, H. & Huang, H. Study on multi-level encoding flow for optical storage based on q-ary RLL. *Proc. SPIE* **5966**, 59660X (2005).
4. Wang, R., Wei, J. & Fan, Y. Chalcogenide phase-change thin films used as grayscale photolithography materials. *Opt. Express* **22**, 4973–4984 (2014).
5. Guo, C. F. *et al.* Grayscale photomask fabricated by laser direct writing in metallic nano-films. *Opt. Express* **17**, 19981–19987 (2009).
6. Wuttig, M. & Yamada, N. Phase-change materials for rewriteable data storage. *Nat. Mater.* **6**, 824–832 (2007).
7. Eggleton, B. J., Luther-Davies, B. & Richardson, K. Chalcogenide photonics. *Nat. Photonics* **5**, 141–148 (2011).
8. Hosseini, P., Wright, C. D. & Bhaskaran, H. An optoelectronic framework enabled by low-dimensional phase-change films. *Nature* **511**, 206–211 (2014).
9. Zhang, X. & Wei, J. Direct detection of the transient superresolution effect of nonlinear saturation absorption thin films. *Photon. Res.* **3**, 100–105 (2015).
10. Shportko, K. *et al.* Resonant bonding in crystalline phase-change materials. *Nat. Mater.* **7**, 653–658 (2008).
11. Wuttig, M. & Salinga, M. Phase-change materials: fast transformers. *Nat. Mater.* **11**, 270–271 (2012).
12. Zhang, K., Lin, J. & Wang, Y. Phase-selective fluorescence of doped $\text{Ge}_2\text{Sb}_2\text{Te}_5$ phase-change memory thin films. *Chin. Opt. Lett.* **13**, 121601 (2015).
13. Wang, Q. *et al.* 1.7 Gbit/in² gray-scale continuous-phase-change femtosecond image storage. *Appl. Phys. Lett.* **104**, 121105 (2014).
14. Fu, J. *et al.* Structural evolution of $\text{Ge}_2\text{Sb}_2\text{Te}_5$ films under the 488nm laser irradiation. *Mater. Lett.* **88**, 148–151 (2012).
15. Zhou, W. P. *et al.* Crystallization of amorphous $\text{Ge}_2\text{Sb}_2\text{Te}_5$ films induced by an ultraviolet laser. *Appl. Surf. Sci.* **285**, 97–101 (2013).
16. Junji, T. & Nobufumi, A. Study of the Crystallization of GeSbTe films by Raman spectroscopy. *Jap. J. Appl. Phys.* **38**, L322 (1999).
17. Satoh, H., Sugawara, K. & Tanaka, K. Nanoscale phase changes in crystalline $\text{Ge}_2\text{Sb}_2\text{Te}_5$ films using scanning probe microscopes. *J. Appl. Phys.* **99**, 024306 (2006).
18. Yoon, H. R., Jo, W., Cho, E., Yoon, S. & Kim, M. Microstructure and optical properties of phase-change Ge–Sb–Te nanoparticles grown by pulsed-laser ablation. *J. Non-Crystal. Solids* **352**, 3757–3761 (2006).
19. Upadhyay, M., Murugavel, S., Anbarasu, M. & Ravindran, T. R. Structural study on amorphous and crystalline state of phase change material. *J. Appl. Phys.* **110**, 083711 (2011).
20. Andrikopoulos, K. S., Yannopoulos, S. N., Kolobov, A. V., Fons, P. & Tominaga, J. Raman scattering study of GeTe and $\text{Ge}_2\text{Sb}_2\text{Te}_5$ phase-change materials. *J. Phys. Chem. Solids* **68**, 1074–1078 (2007).
21. Němec, P. *et al.* Ge–Sb–Te thin films deposited by pulsed laser: An ellipsometry and Raman scattering spectroscopy study. *J. Appl. Phys.* **106**, 103509 (2009).
22. Kozyukhin, S., Veres, M., Nguyen, H. P., Ingram, A. & Kudoyarova, V. Structural changes in doped $\text{Ge}_2\text{Sb}_2\text{Te}_5$ thin films studied by Raman spectroscopy. *Physics Procedia* **44**, 82–90 (2013).
23. Cheng, H. Y., Jong, C. A., Chung, R. J., Chin, T. S. & Huang, R. T. Wet etching of $\text{Ge}_2\text{Sb}_2\text{Te}_5$ films and switching properties of resultant phase change memory cells. *Semi. Sci. Tech.* **20**, 1111–1115 (2005).
24. Zhang, Z. *et al.* Temperature-dependent phase separation during annealing of $\text{Ge}_2\text{Sb}_2\text{Te}_5$ thin films in vacuum. *Appl. Surf. Sci.* **258**, 6075–6079 (2012).
25. Lim, W. S., Cho, S. J. & Lee, H. Y. Change in local atomic and chemical bonding structures of $\text{Ge}_2\text{Sb}_2\text{Te}_5$ alloys by isothermal heat treatment. *Thin Solid Films* **516**, 6536–6540 (2008).
26. Shin, M. J., Choi, D. J., Kang, M. J. & Choi, S. Y. Chemical bonding characteristics of $\text{Ge}_2\text{Sb}_2\text{Te}_5$ for Thin Films. *J. Kor. Phys. Soc.* **44**, 10–13 (2004).
27. Němec, P., Prikryl, J., Nazabal, V. & Frumar, M. Optical characteristics of pulsed laser deposited Ge–Sb–Te thin films studied by spectroscopic ellipsometry. *J. Appl. Phys.* **109**, 073520 (2011).
28. Huang, B. & Robertson, J. Bonding origin of optical contrast in phase-change memory materials. *Phys. Rev. B* **81**, 081204 (2010).
29. Welnic, W., Botti, S., Reining, L. & Wuttig, M. Origin of the optical contrast in phase-change Materials. *Phys. Rev. Lett.* **98**, 236403 (2007).

Acknowledgements

This work was partially supported by the National Natural Science Foundation of China (Nos 51672292, 61627826 and 61137002).

Author Contributions

T.W. wrote the main manuscript text. K.Z. and H.X.Z. checked up and gave some valuable suggestions. J.S.W. and L.Z. were responsible for the experiment. All authors reviewed the manuscript.

Additional Information

Competing financial interests: The authors declare no competing financial interests.

How to cite this article: Wei, T. *et al.* Grayscale image recording on $\text{Ge}_2\text{Sb}_2\text{Te}_5$ thin films through laser-induced structural evolution. *Sci. Rep.* **7**, 42712; doi: 10.1038/srep42712 (2017).

Publisher's note: Springer Nature remains neutral with regard to jurisdictional claims in published maps and institutional affiliations.



This work is licensed under a Creative Commons Attribution 4.0 International License. The images or other third party material in this article are included in the article's Creative Commons license, unless indicated otherwise in the credit line; if the material is not included under the Creative Commons license, users will need to obtain permission from the license holder to reproduce the material. To view a copy of this license, visit <http://creativecommons.org/licenses/by/4.0/>

© The Author(s) 2017